

# **SGK1 Inhibition Induces Fetal Hemoglobin and Delays Polymerization in Sickle Erythroid Cells**

Yannis Hara, Viktor T. Lemgart, Nis Halland, Kiana Mahdaviyani, Jean-Antoine Ribeil, Samuel Lessard, Alexandra Hicks, David R. Light

## **SUPPLEMENTAL MATERIAL**

### **METHODS**

#### **Reagents**

Compound 16y (Comp16y, 5-chloro-2-fluoro-N-[4-[4-[(1-isopropyl-4-piperidyl)oxy]-3-methyl-1H-pyrazolo[3,4-d]pyrimidin-6-yl]phenyl] benzenesulfonamide, supplemental Figure 1) was synthesized as previously described<sup>1</sup>. Hydroxyurea was purchased from Sigma Aldrich.

#### **CD34+ erythroid cell differentiation**

CD34+ cells from healthy donors were purchased from Stemcell Technologies and CD34+ cells from sickle cell blood donors were isolated by CD34+ cell positive selection on PBMC using magnetic beads coupled with an antibody anti-CD34 from Miltenyi Biotech. PBMC were isolated with a Ficoll gradient from whole blood. CD34+ cells from healthy and SCD donors were differentiated in culture as described previously<sup>2,3</sup>. Briefly, mobilized CD34+ human stem / progenitor cells (HSPC) from healthy individuals or CD34+ selected from SCD donor PBMC were cultured for 3 days in a maintenance media consisting of X-VIVO 10 (VWR), 100 U/mL penicillin-streptomycin (ThermoFisher), 2 mM L-glutamine (Fisher Scientific), 100 ng/mL Recombinant Human Stem Cell Factor (SCF), 100 ng/mL Recombinant Human Thrombopoietin (TPO) and 100 ng/mL Recombinant Human Flt-3 Ligand (Flt-3L) (all three from ThermoFisher). Then, cells were differentiated into erythroid cells using a three-step differentiation protocol<sup>3,4</sup>. CD34+ cells were cultured for 7 days in Step 1 media, consisting of Iscove's modified Dulbecco's medium (IMDM) (ThermoFisher) supplemented with 1X GlutaMAX, 100 U/mL penicillin-streptomycin (ThermoFisher), 5% human AB+ plasma, 330 µg/mL human holo-transferrin, 10 µg/mL human insulin, 2 U/mL heparin, 1 µM hydrocortisone (Sigma-Aldrich), 3 U/mL recombinant human erythropoietin (EPO) (ThermoFisher), 100 ng/mL SCF (ThermoFisher) and 5 ng/mL interleukin 3 (IL-3) (Sigma Aldrich). On day 7, cells were

transferred to step 2 media, a step 1 media without hydrocortisone and IL-3, and cultured for 3 to 4 days. Then cells were cultured for 8 to 9 days in step 3 media, a step 2 media without SCF. During CD34<sup>+</sup> differentiation the potent and highly selective SGK1 inhibitor Compound 16y (Comp16y), derived from the exploration of potent and selective SGK1 inhibitors<sup>5</sup> and published previously<sup>1</sup>, was used to inhibit SGK1 at a final concentration of 5  $\mu$ M Comp16y from day 0 to day 21 of differentiation and compared with DMSO (0.1% final) as vehicle control. A concentration of 5  $\mu$ M has been previously determined in cell-based activity assays as sufficient to achieve complete SGK1 inhibition.

### **Flow cytometry**

To determine the percentage of HbF-positive cells (F-cells), differentiated cells were fixed and permeabilized using a fixation kit (ThermoFisher). Cells were stained with phycoerythrin (PE)-conjugated anti-CD235 antibody (ThermoFisher) and anti-CD71 (Thermofisher). HbF levels were detected using allophycocyanin (APC)-conjugated anti-HbF antibody (ThermoFisher). Acquisition of stained cells was performed on BD FACSCanto™ and analysis run using FlowJo™ Software. To determine the enucleation rate of the erythroid differentiated cells at day 21, cells were stained using living cells marker NucRed (Thermofisher).

### **Western blots**

To measure protein expression, Western blots were performed as described previously<sup>6</sup>. Total cell lysates cells were generated and the total protein concentration was determined using a Bradford protein assay (ThermoFisher Scientific). Reduced and denatured protein (40  $\mu$ g) was loaded and separated by SDS-PAGE (12% gel), blotted on nitrocellulose membranes (BioRad) and finally incubated with antibodies anti-SGK1 (Cell Signaling), anti-FOXO3 (Cell Signaling), anti-Phospho-FOXO3 (Ser413) (Cell Signaling), anti-Phospho-SGK1 (Thr-256) (Bioss), anti-human  $\gamma$ -globins ( $\gamma^A$ -globin and  $\gamma^G$ -globin) (Cell Signaling), anti- $\beta$ -globin (Cell Signaling), anti-Band-3 (Cell Signaling), anti-LRF (Abcam), anti-ALAS2 (Abcam), anti-GATA-1 (Cell Signaling) and anti- $\alpha$ -tubulin (Cell Signaling). The  $\alpha$ -tubulin antibody served as an internal control. Immunoreactive proteins were visualized by using an ECL® (enhanced chemiluminescence) detection system (BioRad). Optical density was measured with ImageJ software (National Institutes of Health, Bethesda, MD)

### **Sickling assay**

Sickling of fully differentiated CD34+ PBMC erythroid cells from SCD blood donors under hypoxia was analyzed on day 21 using a sickle cell imaging flow cytometry assay (SIFCA)<sup>7,8</sup> as described previously<sup>6</sup>. Differentiated SCD donor CD34+ cells were challenged under hypoxic conditions by suspending  $5 \times 10^5$  cells in 400  $\mu$ L of Hemox buffer (TCS Sci Corporation) and incubating under 2% oxygen for 4 hours in a 24-well plate with a control plate incubated under normoxia. After incubation, cells were fixed with 40  $\mu$ L of 25% EM grade freshly thawed glutaraldehyde (Sigma Aldrich) and maintained in their original conditions of hypoxia or normoxia for an additional 20 minutes. Cells were washed with PBS before analyzing. Cell images were acquired and sorted using an Amnis ImageStream X and shape change was quantitated using IDEAS software (Luminex). Additional images were obtained using a Zeiss microscope at magnification of 20x.

### **HPLC**

Hemoglobins were quantitated by high-performance liquid chromatography (HPLC). CD34+ cells were lysed in MilliQ H<sub>2</sub>O. then hemolysates centrifuged and hemoglobin variants HbF and HbA<sub>0</sub> analyzed by cation-exchange HPLC on a Waters Acquity system with a Thermo ProPac WCX-10 Analytical Column (4  $\times$  250 mm). Proteins were eluted in 20 mM bis-tris pH 6.95 with a 0 to 200 mM NaCl gradient. Hemoglobin peaks absorbing at 410 nm were integrated.

### **Generation of CD34+ cell FOXO3 knockout**

To knockout FOXO3a protein in CD34+ cells, a CRISPR-Cas9 gene editing was conducted at an early stage of differentiation (Day 2). A synthetic Cas9 was purchased from Aldevron and FOXO3a sgRNAs were purchased from Synthego: gRNA-1 – ACTGCCACGGCTGACTGATA- and gRNA-8 – CGTGACGGTGGAACTGCCA-. To transfect the cells with the complex Cas9-gRNA, an electroporation kit optimized for primary erythroid cells transfection (Amaxa, Lonza) was used. Protein silencing was confirmed by Western blot.

### **Giemsa staining**

To assess the cell morphology at Day 14 of differentiation, a Giemsa staining was conducted using a kit from Scytek Laboratories. The staining was performed according to the manufacturer (supplemental Figure 2).

### **Monocyte-derived macrophage differentiation, polarization, and analysis**

Monocytes were isolated from healthy donor PBMC by negative selection with EasySep™ Human Monocyte Isolation Kit (Stemcell Technologies) according to the manufacturer. Purified cells were cultured in non-treated 6-well plates in complete maturation media (RPMI-1640 with 10% FBS, 10 ng/mL macrophage colony-stimulating factor (M-CSF, R&D Systems) and 1 ng/mL granulocyte-macrophage colony-stimulating factor (GM-CSF, R&D Systems) for 6 days for monocyte-derived macrophage (MDM) differentiation. Differentiated MDM were harvested with TrypLE Express (ThermoFisher) and treated with 5 μM Comp16y or DMSO (0.1% final) as vehicle control. MDM cells were stimulated with 50 ng/mL IFN-γ and 10 ng/mL LPS or left unstimulated for 24 hours. MDM were harvested using TrypLE Express for flow cytometric analysis of M1 and M2 surface markers. MDM were blocked for non-specific binding using Human TruStain FcX™ (Biolegend) then incubated at 4°C in the dark for 30 minutes with antibodies mixed in Stain Buffer (BSA, BD Biosciences): PE-CD163 (ThermoFisher), APC-CD86 (Biolegend) and BV421-CD80 (Biolegend). Viability was assessed by Fixable Viability Dye eFluor™ 780 (eBioscience). Acquisition performed on a BD Symphony™ and analysis on FlowJo™ Software (BD Life Sciences). Cytokines secreted by MDM were measured in cell supernatants after polarization using a MSD U-PLEX kit multiplex assay (Meso Scale Diagnostics) according to the manufacturer.

### **Expression of SGK1 across human bone marrow single-cells**

SGK1 expression was quantified in 101,935 single bone marrow cells from 8 independent donors downloaded from publicly available expression data (<https://data.humancellatlas.org/>, Human Cell Atlas). Distribution of average SGK1 expression was analyzed in previously defined hematopoietic stem cell (HSC) or erythroid cell subsets, including HSC, MEP (myeloid-erythroid progenitors) and ERP (erythroid progenitors)<sup>9</sup>. Unique molecular identifier (UMI) counts were normalized separately for each donor using the R package Seurat<sup>10</sup> after filtering

out cells with less than 200 genes detected. Data for each donor was integrated using the Seurat IntegrateData function after identifying anchors. Integrated data was scaled using the ScaleData function. Cell types were assigned to each barcode (single cells) as previously described (<http://www.altanalyze.org/ICGS/HCA/Viewer.php>)<sup>9</sup>. The average expression across each cell subset were reported separately for each donor.

### **Quantitative RT-PCR**

Total RNA from CD34+ cells was prepared using a RNeasy Mini kit (Qiagen). A quantity of 1 µg of mRNA was reverse transcribed using an iVILO Retro Transcription kit (ThermoFisher) and 50 ng of the resulting cDNA was amplified by Taqman amplification in a QuantStudio thermocycler (Life Technologies) using HBG (human  $\gamma$ -globin primer) and HBB (human  $\beta$ -globin primer) as genes of interest with GAPDH (mouse gapdh primers) as a housekeeping gene (Life Technologies). The delta Ct was calculated and difference in mRNA expression was expressed as the fold-change relative to vehicle.

## **SUPPLEMENTAL RESULTS**

### **Inhibition of SGK1 decreases pro-inflammatory macrophage polarization**

Treatment of human monocyte-derived macrophages with Comp16y during M1 polarization *in vitro* results in anti-inflammatory M2 macrophages based on decreased CD80 and CD86 and increased CD163 (supplemental Figure 5). Moreover, levels of secreted pro-inflammatory cytokines IL-6 and IL-12p70 were decreased (supplemental Figure 6), with no significant difference between cytokines secreted by nonactivated control cells and activated cells treated with Comp16y. SCD is a chronic inflammatory disease<sup>11</sup> with sterile vascular inflammation driven by hypoxia, RBC hemolysis and release of free heme which activates endothelial and leukocyte TLR4<sup>12</sup> and macrophages<sup>13</sup>. Targeting adhesion molecules on activated leukocytes in SCD is supported by *in vitro* studies<sup>14</sup> and clinical demonstration of lowered VOC following inhibition of leukocyte adhesion<sup>15</sup>. SCD hemolysis increases pro-inflammatory M1 macrophages<sup>13</sup> to initiate pulmonary hypertension (PH)<sup>16</sup> where SGK1 increases macrophage infiltration<sup>17</sup>. While M2 polarized macrophages support vascular remodeling during recovery from hypoxia and hemoglobin triggered PH<sup>18</sup>, emphasizing the importance of our observation that Comp16y switches macrophages from the M1 to M2 phenotype.

## SUPPLEMENTAL FIGURES

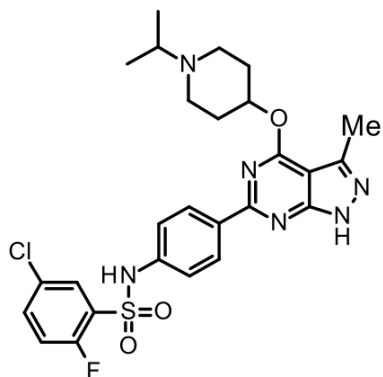


**Figure 1** - SGK1 was inhibited in these studies by Comp16y (Comp16y, 5-chloro-2-fluoro-N-[4-[4-[(1-isopropyl-4-piperidyl)oxy]-3-methyl-1H-pyrazolo[3,4-d]pyrimidin-6-yl]phenyl] benzenesulfonamide), a selective and potent inhibitor of SGK1 ( $IC_{50} = 2$  nM in 10  $\mu$ M ATP, 3 nM in 500  $\mu$ M ATP and 70 nM in mouse chondrogenic ATDC5 cells). In addition, Comp16y shows a promising preclinical pharmacokinetic profile in C57BL/6 mice when dosed orally at 30 mg/kg with a plasma  $C_{max} = 2.2$   $\mu$ g/mL (3.9  $\mu$ M), a plasma  $T_{1/2} = 4.8$  hour and high oral bioavailability  $F\% = 72\%$  <sup>1</sup>.

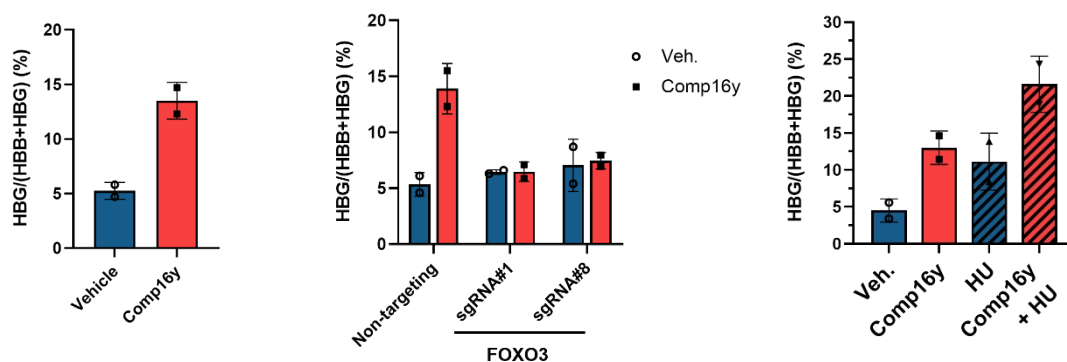


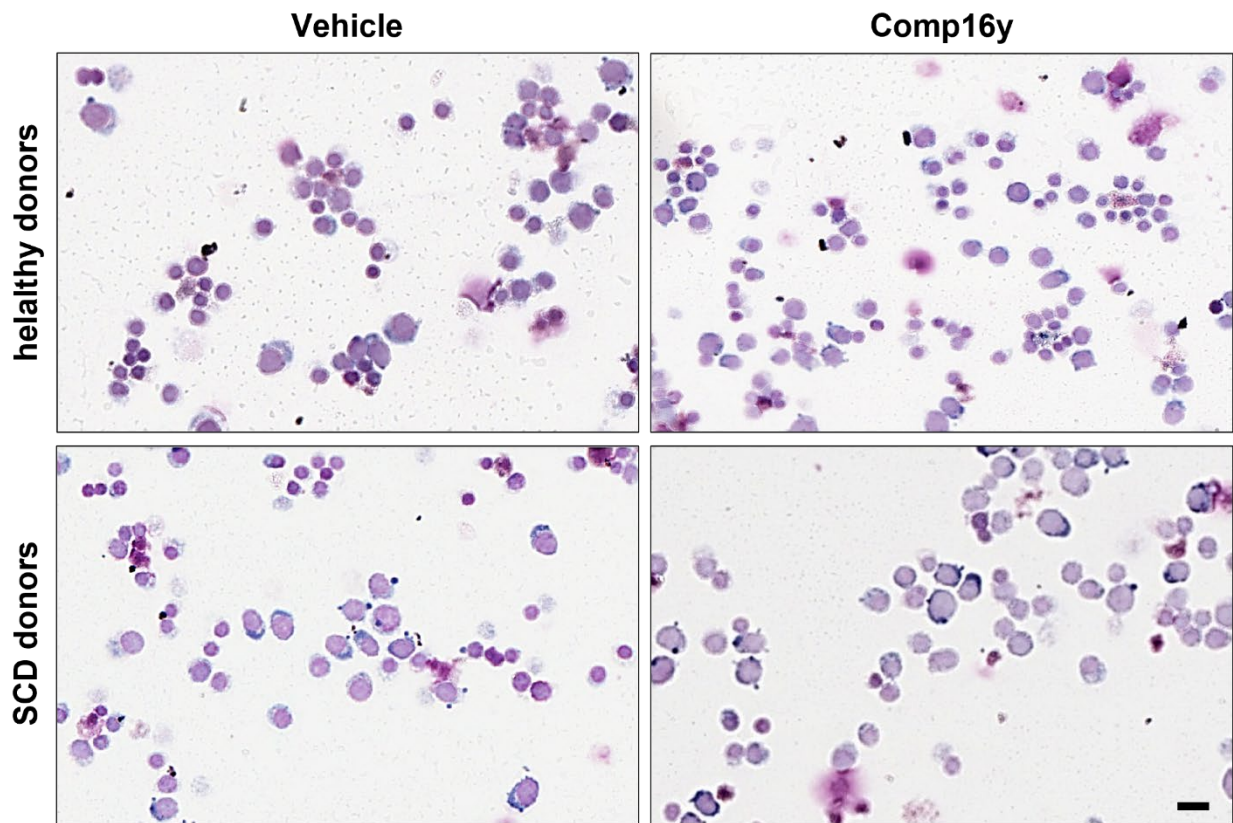
**Figure 2** - human  $\gamma$ -globin (HBG) and human  $\beta$ -globin (HBB) gene expression in CD34+ cells were measured by RT-qPCR and plotted as the ratio HBG/(HBB+HBB). (N=2 independent experiments).

	HbF (%)	HbA (%)	HbA+HbF (%)	HbF/(HbF+HbA) (%)
Vehicle	3.4	72.4	75.8	4.5
Comp16y	16.2	57.8	74	21.9
Comp16y + FOXO3 sgRNA#1	4.6	66.2	70.8	6.5
Comp16y + FOXO3 sgRNA#8	3.3	66.5	69.8	4.7

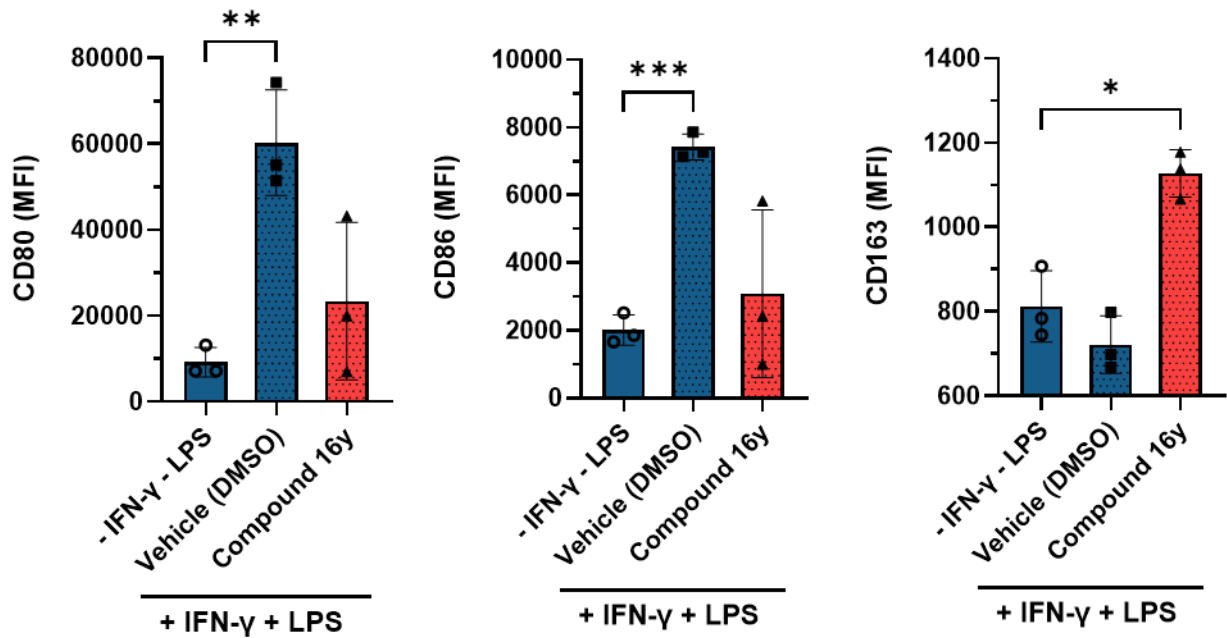
  

	HbF (%)	HbA (%)	HbA+HbF (%)	HbF/(HbF+HbA) (%)
Vehicle	3.3	69.1	72.4	4.6
Comp16y	17.8	59.8	77.6	22.9
HU	6.5	52.4	58.9	11.0
Comp16y + HU	19.8	41.1	60.9	32.5

**Figure 3** - High-performance liquid chromatography (HPLC) analysis of CD34+ cells after treatments with Comp16y.



**Figure 4** - Giemsa staining of differentiated CD34+ cells from healthy and SCD donors, treated with Comp16y for 14 days, confirms normal cell morphologies following treatment with Comp16y (scale bar is 20  $\mu$ m).



**Figure 5** - Treatment of human monocyte-derived macrophages from healthy donors with Comp16y during interferon- $\gamma$  and LPS mediated M1 polarization *in vitro* results in anti-inflammatory macrophages based on decreases in CD80 and CD86 and increases in CD163. Two-tailed t-test, \*\*\* $P < 0.005$ , \*\* $P < 0.01$ , \* $P < 0.05$  (N=3).

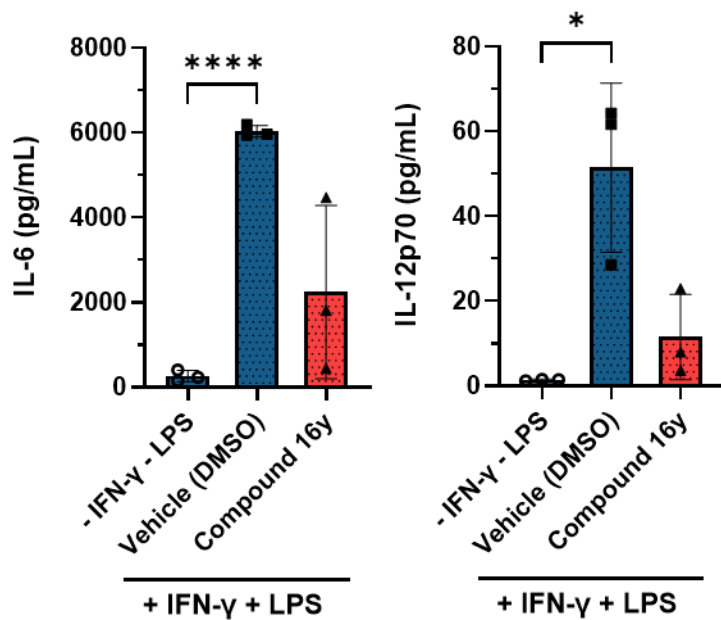


**Figure 6** - Release of inflammatory cytokines IL-6 and IL-12p70 is decreased during M1 polarization of human macrophages treated with Comp16y. Two-tailed t-test, \*\*\*\* $P < 0.001$ , \* $P < 0.05$  (N=3).



## SUPPLEMENTAL REFERENCES

1. Halland N, Schmidt F, Weiss T, et al. Rational Design of Highly Potent, Selective, and Bioavailable SGK1 Protein Kinase Inhibitors for the Treatment of Osteoarthritis. *J Med Chem.* 2022;65(2):1567-1584.
2. Demers M, Sturtevant S, Guertin KR, et al. MetAP2 inhibition modifies hemoglobin S to delay polymerization and improves blood flow in sickle cell disease. *Blood Adv.* 2021;5(5):1388-1402.
3. Giarratana MC, Kobari L, Lapillonne H, et al. Ex vivo generation of fully mature human red blood cells from hematopoietic stem cells. *Nat Biotechnol.* 2005;23(1):69-74.
4. Chang KH, Smith SE, Sullivan T, et al. Long-Term Engraftment and Fetal Globin Induction upon BCL11A Gene Editing in Bone-Marrow-Derived CD34(+) Hematopoietic Stem and Progenitor Cells. *Mol Ther Methods Clin Dev.* 2017;4:137-148.
5. Halland N, Schmidt F, Weiss T, et al. Discovery of N-[4-(1H-Pyrazolo[3,4-b]pyrazin-6-yl)-phenyl]-sulfonamides as Highly Active and Selective SGK1 Inhibitors. *ACS Med Chem Lett.* 2015;6(1):73-78.
6. Krishnamoorthy S, Pace B, Gupta D, et al. Dimethyl fumarate increases fetal hemoglobin, provides heme detoxification, and corrects anemia in sickle cell disease. *JCI Insight.* 2017;2(20).
7. Fertrin KY, Samsel L, van Beers EJ, Mendelsohn L, Kato GJ, McCoy JP, Jr. Sickle Cell Imaging Flow Cytometry Assay (SIFCA). *Methods Mol Biol.* 2016;1389:279-292.
8. van Beers EJ, Samsel L, Mendelsohn L, et al. Imaging flow cytometry for automated detection of hypoxia-induced erythrocyte shape change in sickle cell disease. *Am J Hematol.* 2014;89(6):598-603.
9. Hay SB, Ferchen K, Chetal K, Grimes HL, Salomonis N. The Human Cell Atlas bone marrow single-cell interactive web portal. *Exp Hematol.* 2018;68:51-61.
10. Stuart T, Butler A, Hoffman P, et al. Comprehensive Integration of Single-Cell Data. *Cell.* 2019;177(7):1888-1902 e1821.
11. Zhang D, Xu C, Manwani D, Frenette PS. Neutrophils, platelets, and inflammatory pathways at the nexus of sickle cell disease pathophysiology. *Blood.* 2016;127(7):801-809.
12. Sundd P, Gladwin MT, Novelli EM. Pathophysiology of Sickle Cell Disease. *Annu Rev Pathol.* 2019;14:263-292.
13. Vinchi F, Costa da Silva M, Ingoglia G, et al. Hemopexin therapy reverts heme-induced proinflammatory phenotypic switching of macrophages in a mouse model of sickle cell disease. *Blood.* 2016;127(4):473-486.
14. White J, Krishnamoorthy S, Gupta D, et al. VLA-4 blockade by natalizumab inhibits sickle reticulocyte and leucocyte adhesion during simulated blood flow. *Br J Haematol.* 2016;174(6):970-982.
15. Ataga KI, Kutlar A, Kanter J, et al. Crizanlizumab for the Prevention of Pain Crises in Sickle Cell Disease. *N Engl J Med.* 2017;376(5):429-439.
16. Buehler PW, Swindle D, Pak DI, et al. Murine models of sickle cell disease and beta-thalassemia demonstrate pulmonary hypertension with distinctive features. *Pulm Circ.* 2021;11(4):20458940211055996.
17. Xi X, Zhang J, Wang J, et al. SGK1 Mediates Hypoxic Pulmonary Hypertension through Promoting Macrophage Infiltration and Activation. *Anal Cell Pathol (Amst).* 2019;2019:3013765.

18. Karoor V, Swindle D, Pak DI, et al. Evidence supporting a role for circulating macrophages in the regression of vascular remodeling following sub-chronic exposure to hemoglobin plus hypoxia. *Pulm Circ.* 2021;11(4):20458940211056806.